Slow photoelectron velocity-map imaging spectroscopy of cold negative ions

Christian Hock, Jongjin B. Kim, Marissa L. Weichman, Tara I. Yacovitch, and Daniel M. Neumark[a)]
Department of Chemistry, University of California, Berkeley, California 94720, USA and Chemical Science Division, Lawrence Berkeley National Laboratory, Berkeley, California 94720, USA

(Received 16 October 2012; accepted 30 November 2012; published online 26 December 2012)

Anion slow photoelectron velocity-map imaging (SEVI) spectroscopy is a high-resolution variant of photoelectron spectroscopy used to study the electronic and geometric structure of atoms, molecules, and clusters. To benefit from the high resolution of SEVI when it is applied to molecular species, it is essential to reduce the internal temperature of the ions as much as possible. Here, we describe an experimental setup that combines a radio-frequency ion trap to store and cool ions with the high-resolution SEVI spectrometer. For C_5^-, we demonstrate ion temperatures down to 10 ± 2 K after extraction from the trap, as measured by the relative populations of the two anion spin-orbit states. Vibrational hot bands and sequence bands are completely suppressed, and peak widths as narrow as 4 cm^{-1} are seen due to cooling of the rotational degrees of freedom. © *2012 American Institute of Physics*. [http://dx.doi.org/10.1063/1.4772406]

I. INTRODUCTION

Anion photoelectron spectroscopy (PES) is a versatile tool that can address numerous fundamental topics in spectroscopy and chemical dynamics. It is widely used to investigate the electronic and geometric structure of molecules and clusters.[1–7] PES is an excellent probe of the energetic and spectroscopic effects associated with stepwise solvation of anionic species ranging from single electrons to biomolecules.[8–15] Moreover, as long as suitable geometric constraints are satisfied, anion PES can directly probe the transition state region for a neutral bimolecular or unimolecular reaction, yielding vibrationally resolved spectra of the neutral transition state.[16,17]

Several years ago, anion slow electron velocity-map imaging (SEVI), a high-resolution variant of PES based on photoelectron imaging,[18] was developed in our laboratory.[19,20] For atomic systems, the energy resolution is about 2.5 cm^{-1}. For comparison, the resolution in conventional anion PES with a dispersive electron energy spectrometer is typically 80–100 cm^{-1}, although Cavanagh *et al.*[21] have recently improved upon this using photoelectron velocity-map imaging. The increased resolution of SEVI has yielded new insights into the potential energy surfaces for benchmark bimolecular reactions[22,23] as well as the electronic and geometric structure of molecules and small clusters.[24–26] However, peak widths in the SEVI spectra of molecular anions and clusters have typically been 20–25 cm^{-1}, considerably broader than the spectra of atomic systems. In this paper, we show that the effective resolution of SEVI can be markedly improved by trapping and cooling the negative ions prior to photodetachment.

In the original version of the SEVI experiment, ions were produced by expanding an appropriate gas mixture into vacuum with a pulsed solenoid valve.[27] Anions were created from this expansion by using either an electric discharge or by electron attachment from a pulsed ring anode. In this production scheme, ions are cooled in the free jet expansion after the source, but the efficacy of this cooling, particularly for vibrational degrees of freedom, varies considerably between systems. Incomplete vibrational and rotational cooling can result in spectral congestion that limits the effective resolution of SEVI through a combination of unresolved rotational contours, hot bands originating from excited anion vibrational levels, and unresolved sequence bands.

In this article, we report first results obtained after incorporating radio-frequency (RF) ion guides and an ion trap with buffer gas cooling into the SEVI spectrometer to overcome the limitations mentioned above. The experimental apparatus will be described in detail. Special emphasis is given to the RF trap which is essential for the accumulation and thermalization of the ions. We note that other laboratories have performed conventional photoelectron spectroscopy with ions cooled in a trap prior to photodetachment;[15,28] here we show that the benefits of active cooling are particularly pronounced when combined with the high intrinsic resolution of SEVI.

The capabilities of the instrument are demonstrated for the linear carbon cluster anion C_5^-. The photoelectron spectrum[29,30] and zero electron kinetic energy (ZEKE) spectrum[31] of this species have been reported previously. The ZEKE spectrum showed that C_5^- has a spin-orbit splitting of about 25 cm^{-1} in its $\tilde{X}^2\Pi_u$ ground state; the resolution of ZEKE is sufficient to resolve the two peaks originating from the two anion spin-orbit levels. In the work reported here, the intensities of these two peaks serve as a sensitive and convenient probe of the temperature of the anions extracted from the ion trap, assuming thermalization among the internal degrees

a)Author to whom correspondence should be addressed. Electronic mail: dneumark@berkeley.edu.

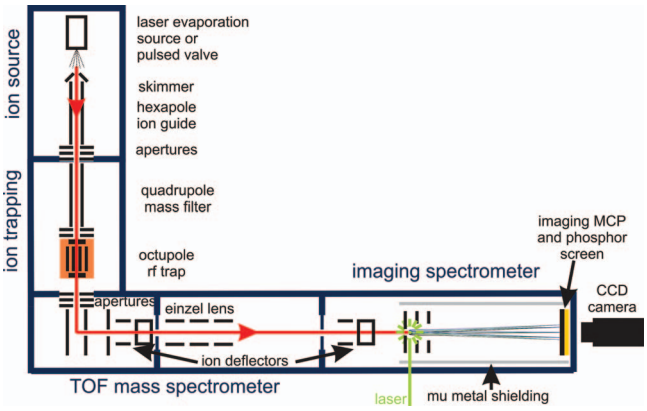

FIG. 1. Schematic of the experimental apparatus.

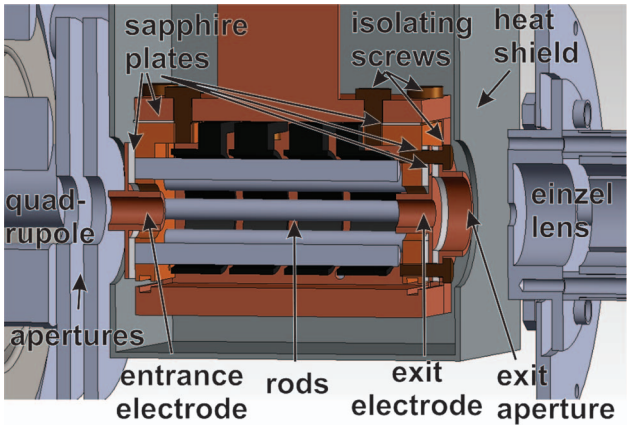

FIG. 2. Sectional view of the octupole ion trap and the surrounding ion optics.

of freedom. We demonstrate that an ion temperature as low as 10 K can be achieved and that under these conditions, peak widths as narrow as 4 cm^{-1} are obtained.

II. EXPERIMENTAL SETUP

A schematic of the experimental setup is shown in Figure 1. The apparatus can be divided into the following differentially pumped sub-units: ion source, ion trap, time-of-flight mass spectrometer (TOFMS), and slow photoelectron velocity-map imaging (SEVI) spectrometer.

The ion source comprises a pulsed solenoid valve[27] that can be coupled to a laser vaporization cluster source,[32] a grid-based electrical discharge,[33] or a pulsed ionizer. The source region is pumped by a turbomolecular pump (Seiko Seiki 2000 L/s). In the work reported here, the C_5^- anions are generated using the laser vaporization source, in which the sample is a 1 in. diameter disc of graphite. To guarantee that every laser shot hits a fresh sample surface, the disc is rotated as well as translated by two independent motors.[34] A frequency doubled Nd:YAG laser is used to vaporize the sample. The laser repetition rate is 20 Hz and the laser power is typically about 2 mJ/pulse at 532 nm. The resulting pulsed jet passes through a skimmer whose potential relative to the source can be adjusted, a RF hexapole ion guide (Ardara Technologies RF power supply, $f = 3$ MHz, typical RF voltage is 200 Vpp, typical bias voltage is 0–5 V), and three electrostatic apertures, all of which are in the source region. The ion guide and apertures efficiently transfer the ions into a quadrupole ion guide located in the differentially pumped ion trapping region. The quadrupole can either be used as a simple ion guide or be operated in a mass-selective mode (Ardara Technologies quadrupole power supply, $f = 1.15$ MHz, typical bias voltage +10 V). After the quadrupole, the ion beam is focused by means of two electrostatic apertures into the RF ion trap.

The ion trap is a linear multipole trap, which has become an indispensable tool in low-temperature experiments on the spectroscopy and kinetics of free charged particles.[35–39] In contrast to many of these experiments, where laser interactions or ion-molecule reactions take place within the ion trap, our experiment requires efficient transfer of the ions into the subsequent TOFMS without heating the ions during extraction. This capability is important since the quality of the SEVI spectra depends on the ion intensity and temperature in the interaction region of the imaging spectrometer.

A sectional view of the ion trap and its surrounding ion optics is presented in Figure 2. The design is similar to that described by Hock *et al.*[39] Trapping in the radial direction is achieved by applying alternating RF voltages to neighboring rod electrodes (Ardara Technologies RF power supply $f = 3$ MHz, maximum voltage 500 Vpp, typical bias voltage −2 V). To confine the ions axially, two electrodes with 6 mm diameter apertures are positioned at the entrance and exit of the trap and are maintained at low negative voltages, typically ≤ -5 V relative to the bias voltage of the RF rods. We use an octupole configuration instead of higher order multipole traps used in previous work[35,36,38,39] for two reasons. First, for the given inscribed diameter D_0 of our RF rods (∼14 mm), the optimum rod diameter d_0 to model an ideal octupole is about 4.75 mm.[35] This allows for a more robust design and easier alignment than higher order multipole traps ($D_0 = 10$ mm, $d_0 = 1$ mm for a 22 pole trap). Second, the effective radial field of an ideal multipole is $V_{eff}(r) \propto r^{n-2}$, where r is the radius and n is the number of rods. Therefore, an octupole has a radial effective field that is proportional to r^6 instead of r^{20} for a 22 pole. The greater curvature of the radial potential in the octupole trap should confine the ions more strongly along the trap axis, facilitating efficient extraction of the ions through the exit aperture.

The ion trap is encased in a copper block that is in good thermal contact with a closed-cycle refrigerator (Sumitomo RDK-408D2; 1 W cooling power at 4 K). The temperature of the ion trap is measured with a calibrated silicon diode (Lakeshore DT-670-SD) and can be adjusted between 5 K and 350 K. To maintain electrical insulation between the different electrodes, sapphire plates were used owing to their very high heat conductivity at cryogenic temperatures. We also use thin indium foil layers between the copper constituents and the sapphire plates to ensure a good thermal contact. The ions are stored inside the trap for 30–45 ms. During this time, they undergo collisions with helium and hydrogen buffer gas (80:20 mixture). The trap is filled with a burst of the buffer gas using a pulsed valve that is supplied through a vacuum gas regulator (pulse width ∼ 300 μs, backing pressure

$\sim$ 7 kPa). The valve is held at room temperature, but the buffer gas is precooled to about 40 K by passing it through a 4 cm long, 4 mm inner diameter tube that is in good thermal contact with the first stage of the closed-cycle refrigerator. Pulsing the buffer gas allows for the trap to be pumped out prior to extraction of the anions, thereby avoiding collisional heating of the ions upon removal from the trap.

The vacuum region containing the trap is pumped by a turbomolecular pump (Seiko Seiki 2000 L/s). The base pressure is 3×10^{-8} mbar when the pulsed valve is closed and the trap is cooled to 5 K. During operation, the equilibrium pressure inside the vacuum chamber holding the ion trap is about 3×10^{-6} mbar (corrected pressure for the ion gauge sensitivity of H_2 and He). Accounting for the gas conductance from the ion trap to the chamber, this leads to an estimated pressure inside the trap of 10^{-3} to 10^{-2} mbar, with the ions making 10^3 to 10^4 collisions with the buffer gas.

The thermalized ions are ejected from the ion trap by applying an attractive potential of 5–10 V to the exit electrode for about 500 μs. After exiting the trap, the ions are transferred into another differentially pumped region and are spatially focused with an einzel lens into the extraction region of a perpendicularly mounted TOFMS in the Wiley-McLaren configuration.[40] The TOFMS spatially and temporally focuses the ions into the laser interaction region of the SEVI spectrometer. Here, mass-selected ions are photodetached in the extraction region of a velocity-map imaging (VMI) ion optical stack,[41] using the frequency-doubled laser pulse from a Nd:YAG pumped tunable dye laser (Radiant Dyes NarrowScan) that operates at a repetition rate of 20 Hz. The expanding three-dimensional electron cloud created by photodetachment is then coaxially extracted down a 50 cm flight tube and mapped onto a position-sensitive detector comprising two chevron-mounted micro-channel plates coupled to a phosphor screen. The application of relatively low VMI voltages magnifies the image on the detector and results in preferential detection of slow electrons, leading to a high absolute electron kinetic energy resolution as described in detail previously.[19,20]

The experimental data presented here have been acquired with a new data acquisition system. The phosphor screen is imaged by a CCD camera with a 768 $\times$ 1024 pixel array (IDS UI-2230SE-M). After each laser shot, an image is read out and transferred to a computer for post-processing. Single electron events are analyzed with an event counting algorithm,[42] where the centroid of each electron spot is determined in order to prevent the resolution from being limited by the spot size of a single event or the camera resolution. The computer software was provided by the group of Suits[43] and has been modified for our needs. After evaluation, the events are binned into a 1024 $\times$ 1024 matrix before the original 3D distribution is reconstructed using an inverse-Abel[44] or pBasex[45] method. The presented spectra were obtained by angular integration of the transformed images. Spectra are reported in electron binding energy (eBE), defined as the difference between the photodetachment energy and the electron kinetic energy (eKE). The apparatus was calibrated by recording SEVI images of atomic F^-[46] at several different photon energies.

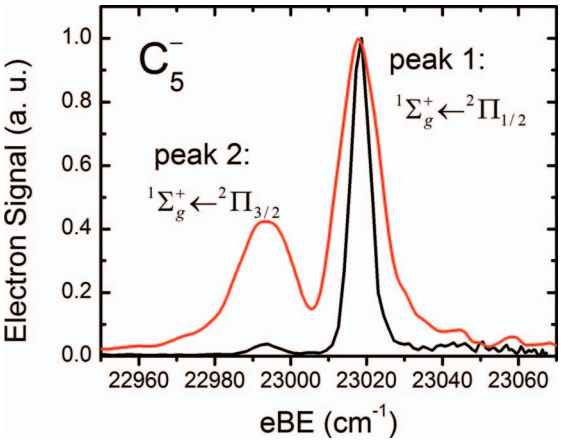

FIG. 3. Comparison of SEVI spectra of C_5^- for different experimental conditions. The spectra show the transitions from the two spin-orbit levels $^2\Pi_{1/2}$ (peak 1) and $^2\Pi_{3/2}$ (peak 2) of C_5^- to the $^1\Sigma^+_g$ state of C_5. The black curve was taken after the ion guiding and trapping system was implemented. The ion trap was held at a temperature of 5 K and the photon energy was 23 068 cm^{-1} (black). The red curve was recorded without the ion trap at 23 105 cm^{-1}. In this case the ions were created in a pulsed solenoid valve and directly injected into the TOFMS. All data has been transformed with the inverse-Abel method.

III. RESULTS AND DISCUSSION

In this section, we will demonstrate that high resolution SEVI spectra can be used to investigate the thermalization of ions by buffer gas cooling inside the RF trap. This is of considerable interest since the temperature of ions stored and thermalized in RF traps is a subject under discussion.[47] We then discuss the effect of cooling and other experimental modifications on the peak widths seen in the SEVI spectrum of C_5^-.

A. Characterization of the ion temperature

A comparison of two SEVI spectra of C_5^- for different experimental setups is presented in Figure 3. The spectra show the transitions from the two spin-orbit levels $^2\Pi_{1/2}$ (peak 1) and $^2\Pi_{3/2}$ (peak 2) of C_5^- to the $^1\Sigma^+_g$ state of C_5, resulting in two peaks separated by about 25 cm^{-1}; both the anion and neutral are in their vibrational ground state. The lower spin-orbit level in the anion (peak 1) results in a peak at higher electron-binding energy. The black curve was recorded after installation of the laser ablation source, ion guide, and ion trapping system. The red curve was taken using the previous configuration of the apparatus, before ion trapping and cooling capabilities were installed. For the red spectrum, the ions were produced by expanding trace amounts of C_2H_2 in argon, at a stagnation pressure of 20–30 bars, into the source vacuum chamber through a pulsed solenoid valve[27] coupled to a grid discharge source.[33] The ions were then directly transferred to a differentially pumped TOFMS through a skimmer and transported to the SEVI spectrometer.

Both spectra are in general agreement with earlier high-resolution measurements on C_5^- that were obtained via ZEKE spectroscopy.[31] However, the signal-to-noise ratio and the energy resolution are significantly better in the SEVI spectra. In both SEVI spectra, the spin-orbit states of C_5^- can be clearly

resolved. Nevertheless, the two spectra differ in two aspects. First, the relative intensities of the two peaks differ greatly for the different experimental setups. Second, the full width at half maximum of the peaks (FWHM) of the spectrum obtained with the ion trap (black curve) is substantially less than for the spectrum without ion trapping (red curve): peak 1 is 6.3 cm^{-1} FWHM compared to 13.3 cm^{-1}, while peak 2 is 8.6 cm^{-1} FWHM compared to 16.8 cm^{-1}.

The relative intensities of peaks 1 and 2 reflect the temperature of the C_5^- prior to photodetachment. Assuming Maxwell-Boltzmann statistics, the relative population of the two states is given by

$$\frac{N_2}{N_1} = e^{-\Delta E/k_b T},$$

where N_1 and N_2 are the integrated intensities of peak 1 and peak 2, ΔE is the energy splitting of the two peaks (25 cm^{-1}), k_b is Boltzmann's constant, and T is the temperature of the system. For the spectrum without the ion trap, we obtain an ion temperature of 59 ± 2 K. This is in good agreement with earlier measurements on C_5^- where the ions were produced with a laser vaporization/pulsed molecular beam source[31] and therefore were also solely cooled by the expansion of the helium carrier gas. The spectrum recorded with the ion trap yields an ion spin-orbit temperature of 10 ± 2 K when the copper block surrounding the ion trap is cooled to 5 K.

It is of interest to estimate the rotational and vibrational temperatures to see if they are consistent with the spin-orbit populations. SEVI cannot resolve individual rovibronic transitions, but the overall rotational profile can limit the line widths in our experiment. For example, peak 1 in Figure 4 has a FWHM of 4.1 cm^{-1} compared to 2.6 cm^{-1} for the F^- detachment at the same eKE. We can simulate the rotational profile for C_5^- using rotational constants derived from calculated, optimized geometries at the RCCSD(T)/aug-cc-pVTZ level of theory for the C_5 anion and neutral. The allowed photodetachment rovibronic transitions[48] are weighted by the Boltzmann population of the anion, and convoluted with a Gaussian with a FWHM of 2.6 cm^{-1} to account for the instrument resolution. The experimental line width is reproduced with a rotational temperature of 14 ± 4 K, which is slightly higher than the nominal spin-orbit temperature, but is consistent within the error bounds. The vibrational temperature can only be roughly estimated since the lowest-frequency ν_7 mode, at 160 cm^{-1}, is barely populated in the temperatures of interest.[49] The 7_1^1 band was previously observed in the ZEKE spectrum,[31] but is not observable above background signal in the current spectra, allowing us to put an upper bound of 40 K for the vibrational temperature. This same experimental setup has been used to suppress hot bands in other systems which will be reported soon. Within the sensitivity of SEVI, the vibrational temperature is consistent with the reported rotational and spin-orbit temperatures.

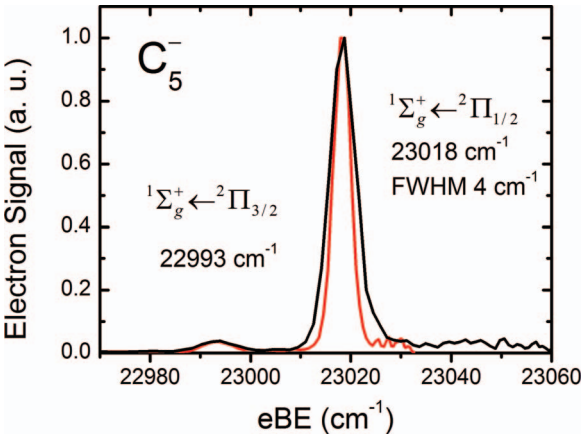

FIG. 4. Comparison of SEVI spectra of C_5^- recorded with the ion trap. As in Figure 3, the spectra show the transitions from the two spin-orbit levels $^2\Pi_{1/2}$ and $^2\Pi_{3/2}$ of C_5^- to the $^1\Sigma^+_g$ state of C_5. The ion trap was held at a temperature of 5 K and the photon energies were 23 068 cm^{-1} (black) and 23 031 cm^{-1} (red). Peak centers and width are given for the red scan. All data have been transformed with the inverse-Abel method.

A concern in this experiment was that extraction of the ions from the trap would lead to collisional heating, resulting in a substantial temperature differential between the ions in the trap and at the point of photodetachment. To ensure that the ions are as close to the nominal trap temperature as possible, it was crucial in our experiment to use the right extraction parameters and to pulse the injection of the buffer gas (see above). We also found that a helium:hydrogen mixture of 80:20 consistently led to lower ion temperatures than using helium gas alone to thermalize the ions. No noticeable dependence on ion temperature was observed when varying the RF amplitude between 150 Vpp and 500 Vpp.

According to Asvany *et al.*,[47] simulations assuming a perfect 22 pole trap can account for a temperature difference of about 4 K between the trap and ion temperature when taking the influence of the RF field, the buffer gas, and a static potential of the entrance and exit electrode into account. Therefore, the results presented here are very close to the optimum thermalization that can be achieved with a linear 22 pole trap, even at the lowest accessible temperature.

The photodetachment cross section σ changes close to threshold depending according to $\sigma \propto (\text{eKE})^{l+1/2}$, where l is the orbital angular momentum of the outgoing electron.[50] For C_5^-, detachment near threshold can proceed by $l = 0$ (s-wave detachment), and the cross section is proportional to $(\text{eKE})^{1/2}$. Since the SEVI spectra are recorded close to threshold, we must ensure that the relative intensities of the two peaks are not dependent on laser wavelength, in order to obtain reliable information about the temperature. For this reason, we have varied the laser wavelength for constant experimental conditions, starting very close to threshold and going to shorter laser wavelengths (higher photon energies) until the resolution of the spectrometer was no longer sufficient to resolve the spin-orbit splitting of C_5^-. All measurements resulted in identical temperatures within the experimental error.

B. Maximizing SEVI resolution via ion trapping and cooling

The narrower peaks in the red spectrum in Figure 3 originate from two effects. First, a new data acquisition system making use of an event counting technique has been used. This will not limit the width of the peaks to the spot size of a single event (discussed above). Second, cooling of the

ions decreases the number of excited rovibrational states in C_5^- and should therefore also reduce the contribution of spectral congestion to the peak widths. Peak widths below 5 cm^{-1} have been achieved in SEVI spectroscopy of atomic anions before implementation of event counting, so we attribute the narrower peak widths mainly to anion cooling.

Since the trapping and cooling of the ions lead to substantially lower ion temperatures, we recorded a spectrum very close to threshold to quantify the best attainable resolution for molecular ions with the improved experimental setup and to derive more accurate energetics for C_5^-. A comparison of two spectra recorded with the ion trap is presented in Figure 4. Again, the transitions from the two $^2\Pi_{1/2}$ and $^2\Pi_{3/2}$ spin-orbit levels of C_5^- to the $^1\Sigma^+_g$ state of C_5 are shown. The peak widths here are even narrower than for the spectrum presented in Figure 3. For peak 1, a FWHM of 4.1 cm^{-1} is reached 13 cm^{-1} from threshold. This is the smallest peak width achieved for any molecular system since the development of the SEVI spectrometer. With this spectrum, we are also able to determine the electron affinity of C_5 to be 23 018(2) cm^{-1}. This is 5 cm^{-1} higher than the previously reported value but well within the error of the earlier measurements.[31] Peak 2 is found at 22 993(3) cm^{-1}. The spacing between the peaks yields a spin-orbit splitting in C_5^- of 25(1) cm^{-1}.

IV. SUMMARY AND OUTLOOK

In this paper, we have described an experimental setup that combines a low-temperature RF ion trap to store and cool ions with a high-resolution SEVI spectrometer. SEVI spectra showing the transitions from the two spin-orbit levels $^2\Pi_{1/2}$ and $^2\Pi_{3/2}$ of C_5^- to the $^1\Sigma^+_g$ state of C_5 are presented. These spectra demonstrate the importance of ion cooling for high-resolution PES. Furthermore, we are able to quantify the temperature of the ions in the interaction region of the imaging spectrometer, i.e., after extraction of the ions from the trap, to be 10 ± 2 K. This low temperature results in a spectral feature with a FWHM of 4.1 cm^{-1} that is measured 13 cm^{-1} above the detachment threshold. The spectra yield a more accurate electron affinity of C_5, 23 018(2) cm^{-1}, and the anion spin-orbit splitting is measured to be 25(1) cm^{-1}.

The combination of the low-temperature ion trap with SEVI opens up the possibility of measuring photoelectron spectra of complex systems with energy resolution comparable to that obtained in the infrared spectroscopy of size-selected ion clusters;[51] recent experiments by Johnson and co-workers[52] have shown that IR spectra of even very large ions become tractable when the ions are cryogenically cooled. The question remains as to whether the approach discussed herein will provide a comparable structural probe of complex species. The selection rules for vibrational transitions are different for infrared and photoelectron spectroscopy, and photoelectron spectra for systems where there is a large geometry change upon photodetachment can be very congested. However, the combination of ion cooling with SEVI is likely to result in well-resolved vibrational structure in systems that, up to now, have yielded only broad features in their photoelectron spectra.

ACKNOWLEDGMENTS

This research is funded by the Air Force Office of Scientific Research under Grant No. FA9550-12-1-0160 and the Defense University Research Instrumentation Program (DURIP) under Grant No. FA9550-11-1-0300. C.H. thanks the German Academic Exchange Service (DAAD) for a postdoctoral scholarship. M.L.W. thanks the National Science Foundation (NSF) for a graduate research fellowship, and T.I.Y. thanks the National Science and Engineering Research Council of Canada (NSERC) for a post-graduate scholarship.

[1] L. A. Posey, M. J. Deluca, and M. A. Johnson, Chem. Phys. Lett. **131**, 170 (1986).
[2] D. G. Leopold, J. Ho, and W. C. Lineberger, J. Chem. Phys. **86**, 1715 (1987).
[3] R. Wester, J. Phys. B **42**, 154001 (2009).
[4] H. Handschuh, C.-Y. Cha, P. S. Bechthold, G. Gantefor, and W. Eberhardt, J. Chem. Phys. **102**, 6406 (1995).
[5] H. Wu, S. R. Desai, and L.-S. Wang, Phys. Rev. Lett. **77**, 2436 (1996).
[6] O. Kostko, B. Huber, M. Moseler, and B. von Issendorff, Phys. Rev. Lett. **98**, 043401 (2007).
[7] C. Bartels, C. Hock, J. Huwer, R. Kuhnen, J. Schwobel, and B. von Issendorff, Science **323**, 1323 (2009).
[8] J. V. Coe, G. H. Lee, J. G. Eaton, S. T. Arnold, H. W. Sarkas, K. H. Bowen, C. Ludewigt, H. Haberland, and D. R. Worsnop, J. Chem. Phys. **92**, 3980 (1990).
[9] G. Markovich, S. Pollack, R. Giniger, and O. Cheshnovsky, J. Chem. Phys. **101**, 9344 (1994).
[10] J. H. Hendricks, S. A. Lyapustina, H. L. de Clercq, J. T. Snodgrass, and K. H. Bowen, J. Chem. Phys. **104**, 7788 (1996).
[11] A. W. Castleman and K. H. Bowen, J. Phys. Chem. **100**, 12911 (1996).
[12] J. Schiedt, R. Weinkauf, D. M. Neumark, and E. W. Schlag, Chem. Phys. **239**, 511 (1998).
[13] M. Mitsui, A. Nakajima, and K. Kaya, J. Chem. Phys. **117**, 9740 (2002).
[14] J. R. R. Verlet, A. E. Bragg, A. Kammrath, O. Cheshnovsky, and D. M. Neumark, Science **307**, 93 (2005).
[15] L. Ma, K. Majer, F. Chirot, and B. von Issendorff, J. Chem. Phys. **131**, 144303 (2009).
[16] K. M. Ervin, J. Ho, and W. C. Lineberger, J. Chem. Phys. **91**, 5974 (1989).
[17] D. M. Neumark, Phys. Chem. Chem. Phys. **7**, 433 (2005).
[18] E. Surber and A. Sanov, J. Chem. Phys. **116**, 5921 (2002).
[19] A. Osterwalder, M. J. Nee, J. Zhou, and D. M. Neumark, J. Chem. Phys. **121**, 6317 (2004).
[20] D. M. Neumark, J. Phys. Chem. A **112**, 13287 (2008).
[21] S. J. Cavanagh, S. T. Gibson, and B. R. Lewis, J. Chem. Phys. **137**, 144304 (2012).
[22] E. Garand, J. Zhou, D. E. Manolopoulos, M. H. Alexander, and D. M. Neumark, Science **319**, 72 (2008).
[23] T. I. Yacovitch, E. Garand, J. B. Kim, C. Hock, T. Theis, and D. M. Neumark, Faraday Discuss **157**, 399 (2012).
[24] J. B. Kim, T. I. Yacovitch, C. Hock, and D. M. Neumark, Phys. Chem. Chem. Phys. **13**, 17378 (2011).
[25] E. Garand, T. I. Yacovitch, J. Zhou, S. M. Sheehan, and D. M. Neumark, Chem. Sci. **1**, 192 (2010).
[26] J. Zhou, E. Garand, and D. M. Neumark, J. Chem. Phys. **127**, 154320 (2007).
[27] U. Even, J. Jortner, D. Noy, N. Lavie, and C. Cossart-Magos, J. Chem. Phys. **112**, 8068 (2000).
[28] X. B. Wang and L. S. Wang, Rev. Sci. Instrum. **79**, 073108 (2008).
[29] S. Yang, K. J. Taylor, M. J. Craycraft, J. Conceicao, C. L. Pettiette, O. Cheshnovsky, and R. E. Smalley, Chem. Phys. Lett. **144**, 431 (1988).
[30] D. W. Arnold, S. E. Bradforth, T. N. Kitsopoulos, and D. M. Neumark, J. Chem. Phys. **95**, 8753 (1991).
[31] T. N. Kitsopoulos, C. J. Chick, Y. Zhao, and D. M. Neumark, J. Chem. Phys. **95**, 5479 (1991).
[32] S. C. O'Brien, Y. Liu, Q. Zhang, J. R. Heath, F. K. Tittel, R. F. Curl, and R. E. Smalley, J. Chem. Phys. **84**, 4074 (1986).
[33] E. Garand, T. I. Yacovitch, and D. M. Neumark, J. Chem. Phys. **130**, 064304 (2009).
[34] T. R. Taylor, K. R. Asmis, C. Xu, and D. M. Neumark, Chem. Phys. Lett. **297**, 133 (1998).

[35]D. Gerlich, *Advances in Chemical Physics* (Wiley, 1992), pp. 1–176.
[36]O. V. Boyarkin, S. R. Mercier, A. Kamariotis, and T. R. Rizzo, J. Am. Chem. Soc. **128**, 2816 (2006).
[37]S. Trippel, J. Mikosch, R. Berhane, R. Otto, M. Weidemuller, and R. Wester, Phys. Rev. Lett. **97**, 193003 (2006).
[38]O. Asvany, E. Hugo, F. Muller, F. Kuhnemann, S. Schiller, J. Tennyson, and S. Schlemmer, J. Chem. Phys. **127**, 154317 (2007).
[39]C. Hock, M. Schmidt, and B. v. Issendorff, Phys. Rev. B **84**, 113401 (2011).
[40]W. C. Wiley and I. H. McLaren, Rev. Sci. Instrum. **26**, 1150 (1955).
[41]A. Eppink and D. H. Parker, Rev. Sci. Instrum. **68**, 3477 (1997).
[42]B.-Y. Chang, R. C. Hoetzlein, J. A. Mueller, J. D. Geiser, and P. L. Houston, Rev. Sci. Instrum. **69**, 1665 (1998).
[43]M. B. Doyle, C. Abeysekara, and A. G. Suits, http://chem.wayne.edu/suitsgroup/NuACQ.html.
[44]E. W. Hansen and P. L. Law, J. Opt. Sci. Am. A **2**, 510 (1985).
[45]G. A. Garcia, L. Nahon, and I. Powis, Rev. Sci. Instrum. **75**, 4989 (2004).
[46]C. Blondel, C. Delsart, and F. Goldfarb, J. Phys. B **34**, L281 (2001).
[47]O. Asvany and S. Schlemmer, Int. J. Mass. Spectrom. **279**, 147 (2009).
[48]J. C. Xie and R. N. Zare, J. Chem. Phys. **93**, 3033 (1990).
[49]M. Perić, M. Petković, and S. Jerosimić, Chem. Phys. **343**, 141 (2008).
[50]E. P. Wigner, Phys. Rev. **73**, 1002 (1948).
[51]J. M. Headrick, E. G. Diken, R. S. Walters, N. I. Hammer, R. A. Christie, J. Cui, E. M. Myshakin, M. A. Duncan, M. A. Johnson, and K. D. Jordan, Science **308**, 1765 (2005).
[52]E. Garand, M. Z. Kamrath, P. A. Jordan, A. B. Wolk, C. M. Leavitt, A. B. McCoy, S. J. Miller, and M. A. Johnson, Science **335**, 694 (2012).